SIRT1 Inhibits High Glucose–Induced TXNIP/NLRP3 Inflammasome Activation and Cataract Formation

Lili Lian,[1,2] Zhenmin Le,[1,2] Zhenzhen Wang,[1,2] Ying-ao Chen,[1,2] Xiaodong Jiao,[3] Hang Qi,[3] J. Fielding Hejtmancik,[3] Xiaoyin Ma,[1,2] Qinxiang Zheng,[1,2] and Yueping Ren[1,2]

[1]National Clinical Research Center for Ocular Diseases, Eye Hospital, Wenzhou Medical University, Wenzhou, China
[2]State Key Laboratory of Ophthalmology, Optometry and Visual Science, Eye Hospital, Wenzhou Medical University, Wenzhou, China
[3]Ophthalmic Genetics and Visual Function Branch, National Eye Institute, National Institutes of Health, Bethesda, Maryland, United States

Correspondence: J. Fielding Hejtmancik, National Eye Institute, National Institutes of Health, 5625 Fisher's Lane, Room 1N02E, Rockville, MD 20852, USA; hejtmancikj@nei.nih.gov.
Xiaoyin Ma, Qinxiang Zheng, and Yueping Ren, Wenzhou Medical University, 270 Xueyuan West Road, Wenzhou, Zhejiang 325027, China; xyma2015@wmu.edu.cn, qinxiangzheng@wmu.edu.cn, yuepingren@wmu.edu.cn.

LL and ZL contributed equally to the study.

Received: October 1, 2022
Accepted: February 6, 2023
Published: March 7, 2023

Citation: Lian L, Le Z, Wang Z, et al. SIRT1 inhibits high glucose–induced TXNIP/NLRP3 inflammasome activation and cataract formation. *Invest Ophthalmol Vis Sci.* 2023;64(3):16. https://doi.org/10.1167/iovs.64.3.16

Purpose. To determine whether SIRT1 regulates high glucose (HG)–induced inflammation and cataract formation through modulating TXNIP/NLRP3 inflammasome activation in human lens epithelial cells (HLECs) and rat lenses.

Methods. HG stress from 25 to 150 mM was imposed on HLECs, with treatments using small interfering RNAs (siRNAs) targeting NLRP3, TXNIP, and SIRT1, as well as a lentiviral vector (LV) for SIRT1. Rat lenses were cultivated with HG media, with or without the addition of NLRP3 inhibitor MCC950 or SIRT1 agonist SRT1720. High mannitol groups were applied as the osmotic controls. Real-time PCR, Western blots, and immunofluorescent staining evaluated the mRNA and protein levels of SIRT1, TXNIP, NLRP3, ASC, and IL-1β. Reactive oxygen species (ROS) generation, cell viability, and death were also assessed.

Results. HG stress induced a decline in SIRT1 expression and caused TXNIP/NLRP3 inflammasome activation in a concentration-dependent manner in HLECs, which was not observed in the high mannitol–treated groups. Knocking down NLRP3 or TXNIP inhibited NLRP3 inflammasome-induced IL-1β p17 secretion under HG stress. Transfections of si-SIRT1 and LV-SIRT1 exerted inverse effects on NLRP3 inflammasome activation, suggesting that SIRT1 acts as an upstream regulator of TXNIP/NLRP3 activity. HG stress induced lens opacity and cataract formation in cultivated rat lenses, which was prevented by MCC950 or SRT1720 treatment, with concomitant reductions in ROS production and TXNIP/NLRP3/IL-1β expression levels.

Conclusions. The TXNIP/NLRP3 inflammasome pathway promotes HG-induced inflammation and HLEC pyroptosis, which is negatively regulated by SIRT1. This suggests viable strategies for treating diabetic cataract.

Keywords: diabetic cataract, NLRP3 inflammasome, SIRT1, TXNIP

Diabetic cataract (DC) is one of the earliest complications of diabetes mellitus (DM), causing vision impairment and blindness. Patients with DM are five times more likely to develop cataract at an early age compared with those without DM.[1] The DC incidence is predicted to rise steadily with the increasing prevalence of DM, predicted to be 439 million patients worldwide by 2030.[2] Chronic hyperglycemia in the aqueous humor plays a key role in the changes of lens metabolism and formation of DC. While polyol accumulation and nonenzymatic glycation have been classically considered the primary mechanisms of diabetic cataract pathophysiology, sterile inflammation driven by long-term hyperglycemia with overgeneration of reactive oxygen species (ROS), accompanied by associated release of inflammatory mediators, and increased advanced glycation end products have been shown to be important in the pathophysiology of DC.[3–5] NLRP3 inflammasome activation has been reported to be a link between ROS accumulation and inflammation in human lens epithelial cells (HLECs) and cataract animal models stressed with high glucose (HG),[6,7] suggesting that NLRP3 inflammasome and subsequent IL-1β release may participate in DC progression. However, the mechanisms that downregulate the undesired inflammasome activation, to terminate the overactivation and recover homeostasis, remain largely unknown.

Silent information regulator T1 (SIRT1), an NAD-dependent class III protein histone deacetylase, regulates the activity of various transcription factors and cofactors involved in inflammation-associated diseases. It is a vital modulator for redox homeostasis and plays important roles in the regulation of cell survival, apoptosis, and inflammation.[8,9] It improves insulin resistance by reducing oxidative stress and regulating mitochondrial function in the progression of DM, while the disturbance of these conditions promotes the pathogenesis of diabetic complications, including DC.[10] It has been shown that a decline in SIRT1 activity

causes apoptosis of lens epithelial cells and cataract development in diabetic mice,[11] and there is evidence indicating that SIRT1 might be associated with NLRP3 inflammasome activation in hyperglycemic conditions.[12] High glucose induced an increase in ROS generation and NLRP3 inflammasome activity in human umbilical vein endothelial cells (HUVECs), and silencing of SIRT1 aggravated NLRP3 inflammasome-induced inflammation in retinal pigment epithelial cells,[13] while a selective SIRT1 activator markedly reversed HG-induced NLRP3 inflammasome activation and cell death.[14,15] Thus, it is reasonable to speculate that SIRT1 might play a role in modulating NLRP3 inflammasome-associated inflammation in DC, emphasizing the importance of understanding the underlying molecular mechanisms.

As known, NLRP3 inflammasome activation is triggered by its binding to thioredoxin interacting protein (TXNIP).[16,17] TXNIP is able to sense the surge of ROS production and then dissociates from thioredoxin to bind NLRP3 and activates the NLRP3 inflammasome.[16] It mediates hyperglycemia-induced NLRP3 inflammasome activation and consequent cell injury,[18] and HG-induced overexpressions of TXNIP and NLRP3 inflammasome activation appear to be associated with SIRT1 expression level in HUVECs.[13] In order to further investigate the possible role SIRT1 plays in the TXNIP/NLRP3 inflammasome pathway in DC, we examined whether changes in SIRT1 expression levels altered TXNIP/NLRP3 inflammasome activation in a human lens epithelial cell (HLEC) line and rat lenses challenged with HG stress. Our results indicate that upregulation of SIRT1 decreases NLRP3 inflammasome responses in HLECs, which corresponds with the differences in cataract formation in rat lenses cultivated with HG medium.

Materials and Methods

Experimental Animals

Two-month-old male Sprague–Dawley rats were purchased from Jie Si Jie Laboratory in Shanghai, China. The rats were raised in the Wenzhou Medical University animal facility under a standard 12-hour light/12-hour dark cycle and provided standard diet and tap water as desired. All animal experiments were performed in accordance with the ARVO statement for the Use of Animals in Ophthalmic and Vision Research and the approved guidelines of the Wenzhou Medical University Institutional Animal Care and Ethics Committee.

Cell Culture and Treatments

The HLEC line (FHL124) was kindly provided by Dr. J.R. Reddan (Oakland University). The cell line was maintained in HG Dulbecco's modified Eagle's medium (DMEM; 25.0 mM glucose; Gibco, USA) supplemented with 10% fetal bovine serum (FBS), 100 U/mL penicillin, and 0.1 mg/mL streptomycin (Beyotime Biotechnology, China) in a humidified atmosphere at 37°C with 5% CO_2. The cell culture medium was changed every 2 days and passaged at 80% to 90% confluence. The medium was replaced by normal-glucose DMEM (5.5 mM glucose; Gibco) with 2% FBS before HG stimulation. In the normal glucose (NG) group, HLEC medium contained 5.5 mM glucose, while in the HG groups, additional glucose (Sigma-Aldrich, St. Louis, MO, USA; Merck KGaA) was added to bring the final concentration of glucose to 25 to 150 mM. The same gradient concentrations of mannitol (Aladdin, China) were added into the media as osmotic control groups.

MCC950 (MCE, USA), an NLRP3 inflammasome inhibitor, was dissolved in normal-glucose DMEM at a concentration of 1 mM as a storage solution. SRT1720 (Topscience, China), a selective SIRT1 activator, stock solution was prepared in DMSO and at a concentration of 10 mM. The final working concentrations of MCC950 and SRT1720 were 1 µM and 0.5 µM, respectively. The above two compounds were added 1 hour before HG stress.

Small Interfering RNA and Lentiviral Transfection

HLECs were seeded in 6-well plates and transfected with small interfering RNAs (siRNAs) or lentiviral vectors (LVs). The siRNAs (40 nM) were transfected into HLECs using a lipojet transfection kit (SignaGen, USA) according to the manufacturer's protocol. The siRNA sequences were designed and synthesized by Gene Pharma Co., Ltd (Shanghai, China). The pCMV-EGFP-puro vector and pCMV-SIRT1-EGFP-puro vector, which encoded full-length human SIRT1, were obtained from Genechem Co., Ltd (Shanghai, China). HLECs were infected with the lentivirus at a MOI = 100 in the DMEM containing Polybrene (5 g/mL). The HCEC cell line stably overexpressing SIRT1 was obtained by puromycin selection (2 µg/mL). Sequences of the siRNAs are given in the Supplementary Table S1.

Lens Organ Culture In Vitro

The eyeballs of adult male rats were extracted after they were euthanized by intraperitoneal injection of overdose pentobarbital sodium (200 mg/kg). In PBS buffer, the neuroretinas were cut from the optic nerve. The complete rat lenses were isolated without damaging the lens capsule. Transparent lenses were transferred to a 24-well plate and cultured in 5.5 mM glucose DMEM aseptically at a humidified atmosphere at 37°C with 5% CO_2 in the NG group or 150 mM glucose DMEM with or without compound treatments in the experimental groups. In addition, the 150-mM mannitol group was applied as the osmotic control group. Lens opacity was measured and calculated using ImageJ software (National Institutes of Health, Bethesda, MD, USA).

Quantitative RT-PCR

Total RNA was extracted from collected cells and rat lens capsules, including the adherent epithelial cells, by RNA lysis buffer RLT (QIAGEN, Germany) according to the manufacturer's protocol. Then, 0.2 to 2 µg RNA from each sample was reverse transcribed with M-MLV reverse transcriptase (Promega, Madison, WI, USA). Quantitative RT-PCR was performed on a Real-Time PCR Detection System (Applied Biosystems, Waltham, MA, USA) with SYBR Green qPCR Master Mix (Applied Biosystems). Relative mRNA expression levels were determined according to the $2^{-\Delta\Delta Ct}$ method. The sequences of the related primers are provided in Supplementary Table S2.

Western Blot Analysis

HLECs were washed with cold PBS buffer for three times and proteins were extracted from RIPA lysates with protease inhibitor (Beyotime Biotechnology). The concentration of total protein was determined by Bradford protein assay

Investigative Ophthalmology & Visual Science

(Beyotime Biotechnology). The protein samples were then separated on 10% to 12% SDS–polyacrylamide gels and transferred to 0.22-µm nitrocellulose blotting membranes. The membrane was blocked in 5% nonfat milk in TBST at room temperature for 2 hours and incubated with primary antibodies overnight at 4°C. The primary antibodies were as follows: anti-NLRP3 (1:1000, 15101S; Cell Signaling Technology), anti–IL-1β (1:1000, 12703S; Cell Signaling Technology), anti–Cleaved–IL-1β (1:500, 83186; Cell Signaling Technology), anti-SIRT1 (1:1000, ab189494; Abcam), anti-TXNIP (1:1000, 14715s; Cell Signaling Technology), antithioredoxin (1:1000, ab109385; Abcam), anti-GAPDH (1:5000, 5174S; Cell Signaling Technology), anti–β-actin (1:2000, 4967S; Cell Signaling Technology), and anti-GFP (1:1000, AG281; Beyotime Biotechnology). The membranes were washed with TBST for three times and incubated with donkey anti-mouse IgG (H + L) IRDye 800CW (LI-COR, USA) or donkey anti-rabbit IgG (H + L) IRDye 800CW (LI-COR) secondary antibody for 1 hour at room temperature. The protein bands were scanned using a LI-COR machine. Quantitative statistics of protein bands were estimated using ImageJ software.

Cell Viability and Propidium Iodide Staining

Enhanced Cell Counting Kit–8 (CCK8; Beyotime Biotechnology) assay was used to determine cell viability. Briefly, HLECs were seeded to 96-well plates at a cell density of 1×10^4 per well. Appropriate basic medium (100 µL) containing 10% CCK-8 reagent was added, and the plates were evaluated by a multifunctional microplate reader (MD SpectraMax 190; Molecular Devices, San Jose, CA, USA) after 2 hours of incubation at 37°C with 5% CO_2.

Propidium iodide (PI) staining (Beyotime Biotechnology) was used to label apoptotic cells. HLECs were seeded to 12-well plates and washed twice with PBS buffer before adding PI test solution. Cells were stained with PI (20 µg/mL) for 20 minutes at room temperature, then washed with PBS twice and fixed with 4% paraformaldehyde for 20 minutes at room temperature. 4′,6-Diamidino-2-phenylindole (DAPI) staining was used to label the total cell number, and its ratio to PI-positive cells represented the percentage of apoptotic cells.

Measurement of ROS

For cells ROS measurement, a CM-H2DCFDA probe (Invitrogen, Carlsbad, CA, USA C6827) was used to detect ROS generation according to the kit instructions. Briefly, HLECs were seeded to 96-well plates at a cell density of 1×10^4 per well. After incubating the cells with 10 µM CM-H2DCFDA dye for 30 minutes at 37°C, the plates were washed twice with PBS and the fluorescence was quantified using a fluorescence microscope (Axio Observer 3; ZEISS, Germany).

For rat lens epithelial cells, ROS was measured using the GENMED kit (Genmed Scientifics, China) according to the manufacturer's instructions. Briefly, 10-µm-thick unfixed rat lens frozen sections were prepared and incubated with 200 µL GENMED staining solution for 30 minutes at 37°C followed by immediate observation under a fluorescence microscope.

Immunostaining and TUNEL Analysis

For cell immunofluorescence, the HLECs were fixed with 4% paraformaldehyde in PBS at room temperature for 30 minutes and permeabilized with 0.1% Triton X-100 for 10 minutes. For histoimmunofluorescence, the isolated rat lenses were fixed with 4% paraformaldehyde at 4°C for 2 hours. The fixed lenses were then embedded in OCT compound and cut into 10-µm sections. The frozen sections were permeabilized with 0.4% Triton X-100 for 10 minutes at room temperature. The cells and tissue section were blocked by a blocking buffer containing 3% bovine serum albumin and 0.1% Triton X-100 at room temperature for 1 hour. Samples were incubated in primary antibody diluted in blocking buffer overnight at 4°C with the following antibodies at the following concentrations. Primary antibodies were used: anti-NLRP3 (1:300, 15101S; Cell Signaling Technology), anti–IL-1β (1:300, 12703S; Cell Signaling Technology), anti-ASC (apoptosis-associated speck-like protein containing a CARD) (1:200, sc-514414; Santa Cruz Biotechnology); anti-SIRT1 (1:300, ab189494; Abcam); anti-TXNIP (1:300, 18243-1-AP; Proteintech). After washing with PBS three times, the samples were incubated with the corresponding secondary antibodies, Alexa Fluor 488–conjugated donkey anti-rabbit IgG (1:250, ab150077; Abcam) and Alexa Fluor 594–conjugated donkey anti-rabbit IgG (1:300, ab150080; Abcam) for 2 hours at room temperature in the dark.

For TUNEL assays, an in situ cell death detection kit (Roche, Mannheim, Germany) was used according to the manufacturer's protocol. Briefly, 10-µm frozen sections were fixed with 4% paraformaldehyde for 30 minutes and permeabilized with 0.1% Triton X-100 for 2 minutes at room temperature. The samples were then incubated in the prepared TUNEL working solution at 37°C for 1 hour. DAPI was used to label rat lens epithelial nuclei.

Statistical Analysis

All experiments were repeated at least three times, and data are presented as mean ± SD. Statistical analyses were performed using GraphPad Prism 8 (GraphPad Software, La Jolla, CA, USA) with Student's *t*-test or Mann–Whitney *U* test when comparing two groups and one-way ANOVA with Dunnett's post hoc test when comparing more than two groups. A P value <0.05 was considered statistically significant.

Results

HG Induces SIRT1 Decline and TXNIP/NLRP3 Inflammasome Activation

After a 4-hour exposure of HLECs to HG media from 25 to 150 mM, the mRNA levels of *SIRT1* decreased ($P \leq 0.001$) in a concentration-dependent manner, while those of *TXNIP*, *NLRP3*, and *IL-1β* increased significantly ($P \leq 0.016$) (Figs. 1A–D). The Western blot results showed that the protein levels of SIRT1 also declined, while TXNIP, NLRP3, IL-1β, and its bioactive form, p17, rose correspondingly ($P \leq 0.002$), although thioredoxin expression remained unaffected by HG stress (Figs. 1E, 1F). Another indication of NLRP3 inflammasome activation is that ASC immunofluorescence synergized with NLRP3 and IL-1β expression during exposure to the HG medium (Fig. 1G). In addition, ROS production increased by 3.4-fold above the baseline level in medium with 150 mM glucose ($P = 0.003$) (Figs. 1G, 1H). As osmotic controls, high mannitol treatment from 25 to 150 mM also did not cause significant changes in the gene and protein levels of SIRT1 and NLRP3, as well as the bioactive IL-1β p17 secretion (Supplementary Fig. S1). These results

Investigative Ophthalmology & Visual Science

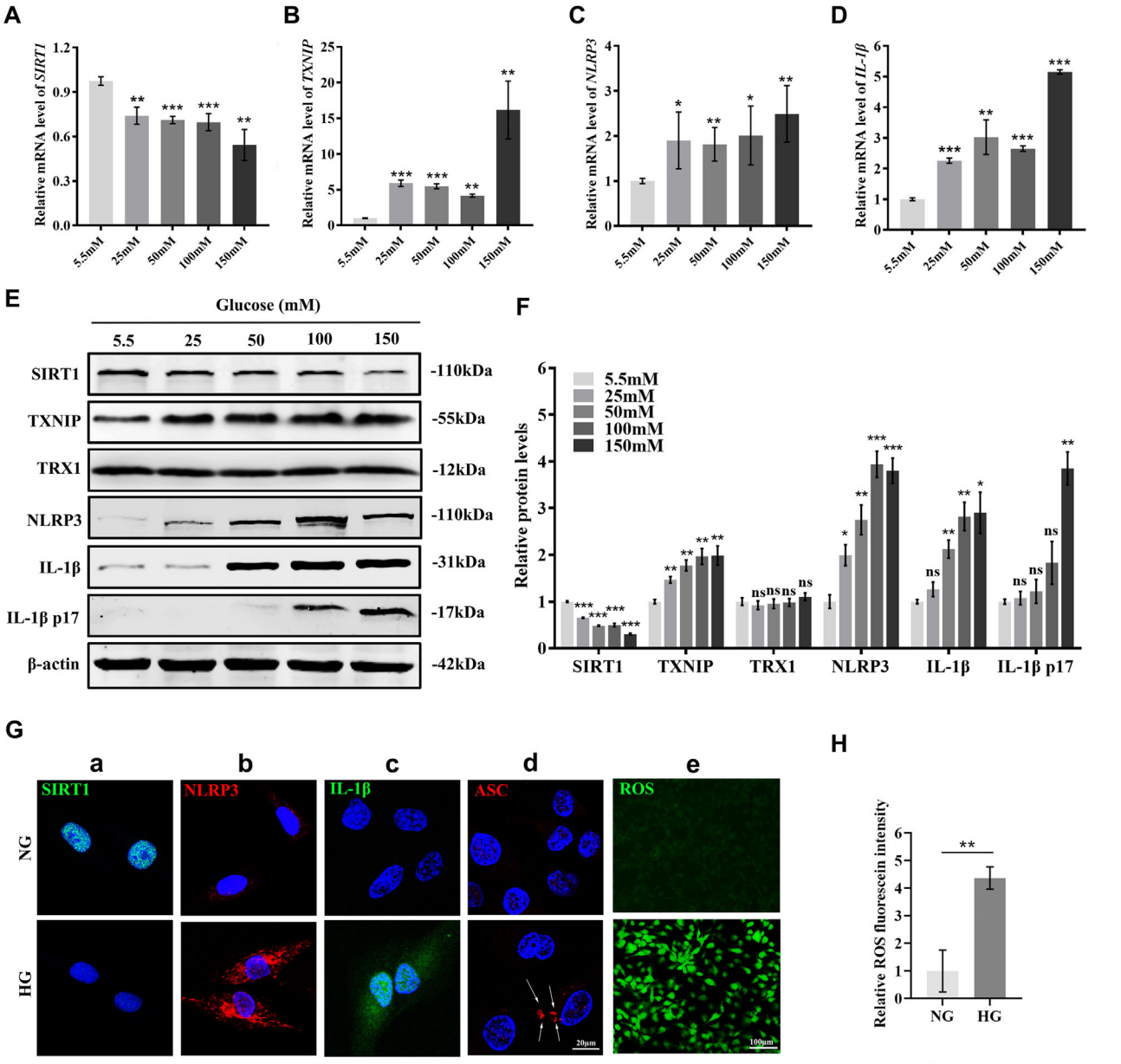

Figure 1. HG induces a decline in SIRT1 expression and TXNIP/NLRP3 inflammasome activation. (**A–D**) After HLECs were treated with different concentrations of glucose (5.5 mM, 25 mM, 50 mM, 100 mM, and 150 mM) for 4 hours, quantitative RT-PCR was performed to assess the mRNA expression of *SIRT1*, *TXNIP*, *NLRP3*, and *IL-1β*. (**E**, **F**) Expression of SIRT1 and TXNIP/NLRP3 inflammasome-associated proteins was detected in the indicated glucose-treated HLECs using WB. The relative protein intensity was expressed and quantified as the ratio of protein level to β-actin protein level. (**G**) Immunofluorescent staining against SIRT1 (**a**), NLRP3 (**b**), IL-1β (**c**), and ASC (**d**) was performed in the control and HG-treated HLECs. ROS level (**e**) was detected in the indicated HLECs by the DCFDA cellular ROS detection assay kit. (**H**) Quantification of ROS level 24 hours after a 150-mM glucose treatment. Data were collected from three separate experiments. $^{*}P < 0.05$, $^{**}P < 0.01$, $^{***}P < 0.001$, as compared with the 5.5-mM glucose group.

demonstrate that HG induces oxidative stress accompanied by a decline in SIRT1 expression, TXNIP/NLRP3 expression, and inflammasome activation in HLECs.

Because TXNIP binding is an essential step for NLRP3 inflammasome activation, we knocked down NLRP3 and TXNIP gene expressions by targeted siRNA transfections to verify their inhibitory effects on NLRP3 inflammasome-induced IL-1β p17 secretion in HG-stressed HLECs. Transfection with si-NLRP3s effectively decreased the mRNA and protein levels of NLRP3 ($P \leq 0.020$) (Figs. 2A–C), which made the secretion of active IL-1β p17 decline significantly ($P \leq 0.027$), while the IL-1β expression remained unaffected (Figs. 2B, 2C). Similarly, transfection of si-TXNIPs also significantly reduced the mRNA and protein expressions of NLRP3 and the release of IL-1β p17 ($P \leq 0.043$) (Figs. 2D–G). Thus, inhibiting TXNIP or NLRP3 expression could effectively suppress the inflammasome-induced bioactive IL-1β release.

In addition, we tested the effects of the NLRP3 protein inhibitor MCC950 on HG-induced inflammatory responses in HLECs for its possible clinical application. It was found that MCC950 significantly suppressed NLRP3 protein levels

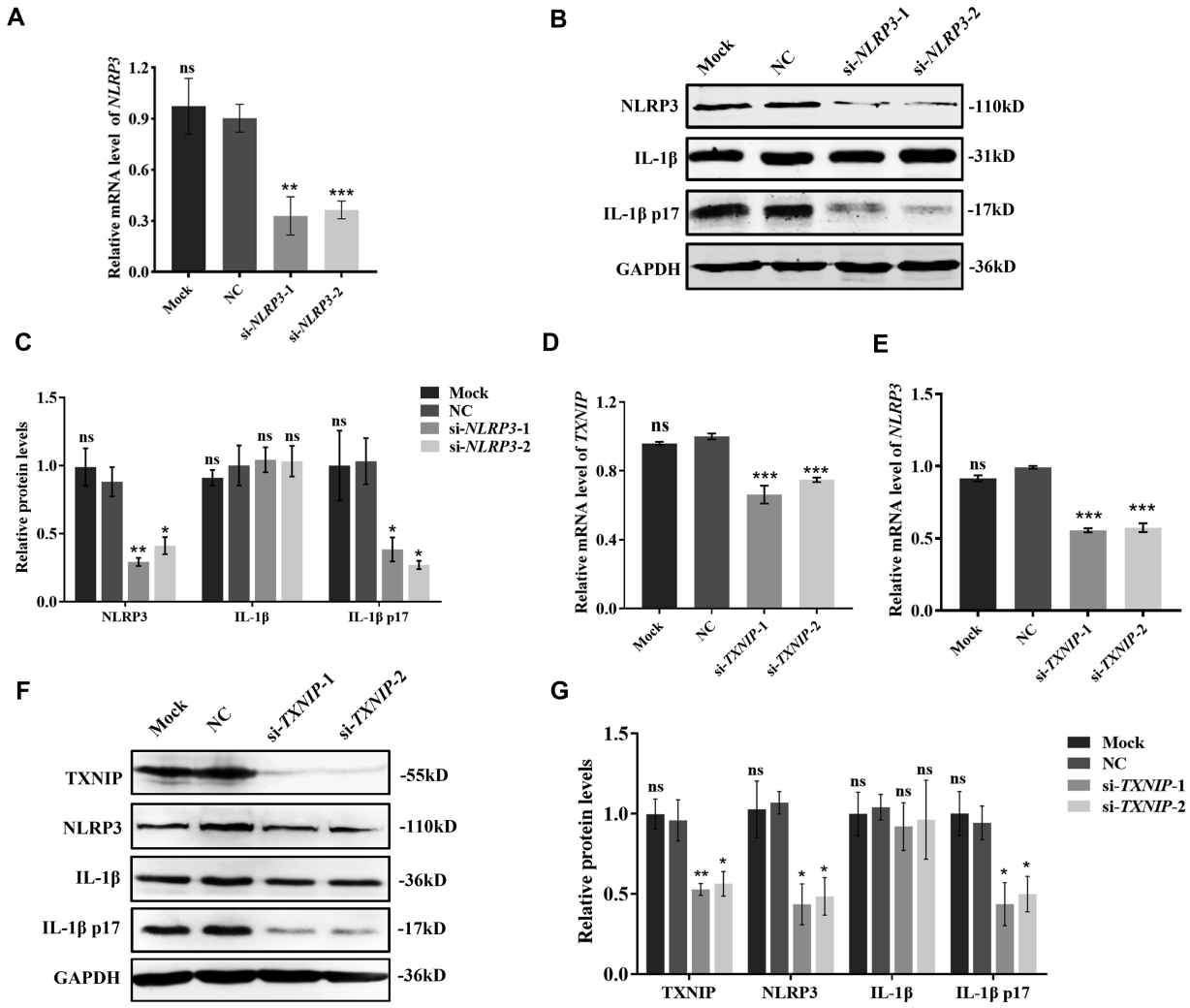

Figure 2. HG-induced pyrotosis depends on the TXNIP/NLRP3 signaling pathway. (**A**) The interference efficiency of NLRP3 siRNAs on the expression of *NLRP3* analyzed via quantitative RT-PCR (qRT-PCR) after 48 hours of transfection. (**B**, **C**) HLECs were transfected with control or NLRP3 siRNAs for 48 hours and then treated with 150 mM glucose for 24 hours. Cells were lysed and immunoblotted with antibodies against NLRP3, IL-1β, IL-1β p17, and GAPDH. (**D**) The interference efficiency of TXNIP siRNAs on the expression of *TXNIP* analyzed via qRT-PCR after 48 hours of transfection. (**E**) HLECs were transfected with control or TXNIP siRNAs for 48 hours and then treated with HG for 24 hours. Relative *NLRP3* mRNA levels were assessed by qRT-PCR. (**F**) HLECs were treated with TXNIP siRNAs and HG as indicated, and cell lysates were subjected to immunoblotting with antibodies against TXNIP, NLRP3, IL-1β, IL-1β p17, and GAPDH. (**G**) Quantification of protein level based on the WB analysis. Data were collected from three separate experiments. *$P < 0.05$, **$P < 0.01$, ***$P < 0.001$; ns, not significant as compared with the control group.

and IL-1β p17 secretion under HG stress ($P \leq 0.031$) (Figs. 3A–D), as well as the expression of ASC (Fig. 3G). Cell viability in the HG group was 75% of that in the normal group ($P = 0.002$) but returned toward normal levels with MCC950 treatment ($P = 0.026$) (Figs. 3E, 3H). The PI results showed that incubation in HG medium dramatically increased cell death ($P = 0.008$), which could be rescued by MCC950 treatment ($P = 0.003$) (Figs. 3F, 3H). The above results suggest that the NLRP3 protein inhibitor MCC950 is an optimal candidate for inhibition of HG-induced NLRP3 inflammasome activation.

SIRT1 Modulates HG-Induced TXNIP/NLRP3 Activation

To assess whether SIRT1 plays a regulatory role in TXNIP/NLRP3 inflammasome activation, we knocked down SIRT1 by transfection of si-SIRT1 and increased SIRT1 expression levels by LVs in HLECs. Transfection of si-SIRT1s significantly inhibited the mRNA and protein levels of SIRT1 ($P \leq 0.007$), while expression of TXNIP and NLRP3 increased inversely ($P \leq 0.001$) (Figs. 4A–E).

Conversely, LV-SIRT1 transfection elevated *SIRT1* mRNA expression levels by more than 4-fold ($P = 0.004$) and the protein level by 2.5-fold ($P = 0.009$) (Figs. 5A, 5E, 5F). When the LV-SIRT1–infected HLECs were challenged with 150 mM HG stress for 4 or 24 hours, the results showed that LV-SIRT1 infection effectively suppressed the increases in TXNIP, NLRP3, and IL-1β mRNA and protein levels (Figs. 5B–F) ($P \leq 0.005$), as well as the ASC assembly (Fig. 5G). LV-SIRT1 infection also restored cell viability nearly twofold compared with those in the HG LV-EGFP group ($P = 0.002$) (Figs. 5H, 5J), and PI results verified its protective role against HG insult ($P = 0.029$)

Investigative Ophthalmology & Visual Science

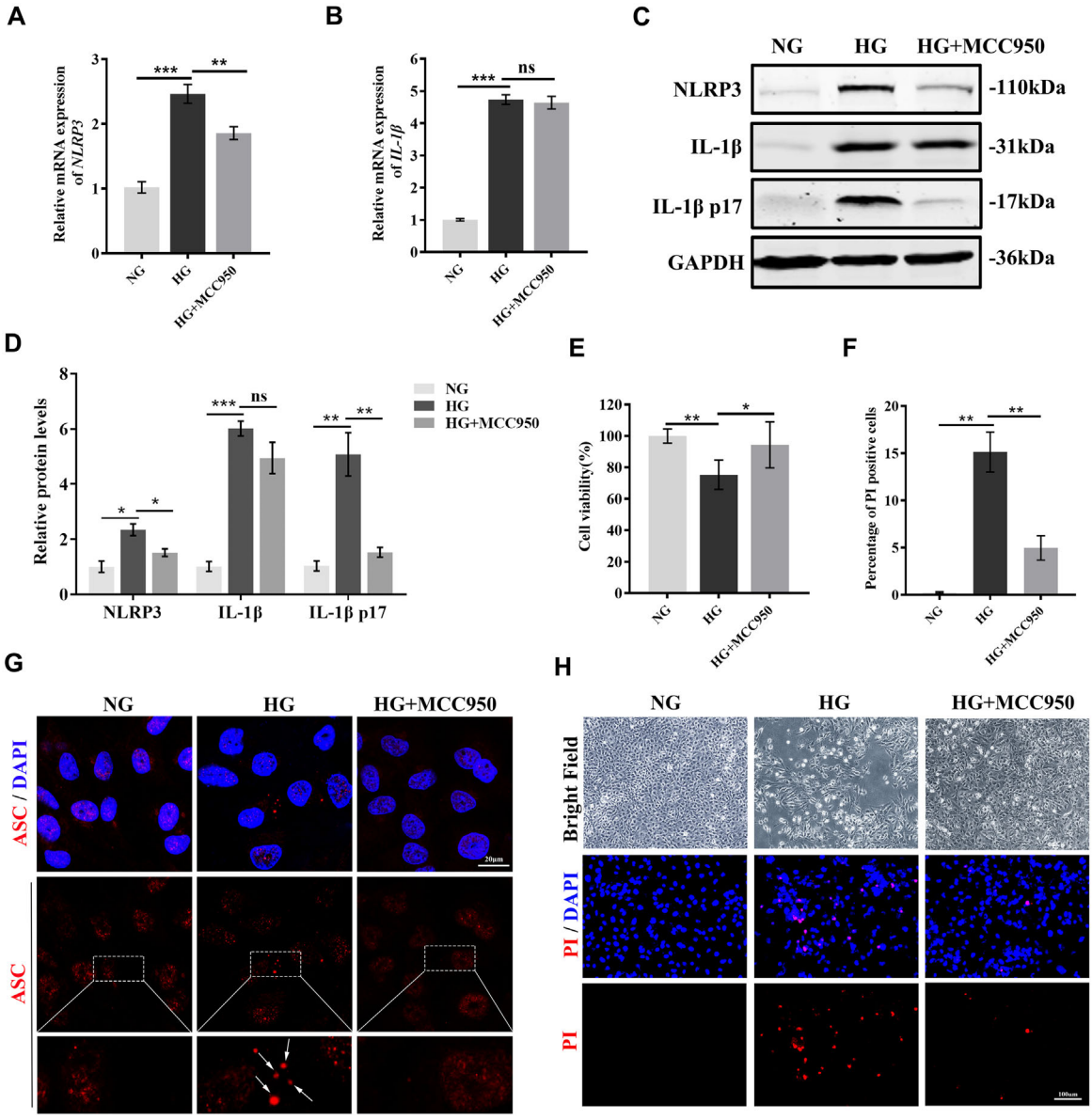

Figure 3. Targeting the NLRP3 inflammasome with the NLRP3 inhibitor MCC950 prevents HG-induced HLEC pyroptosis. Schematic representation of MCC950 treatment experiments. (**A**, **B**) qRT-PCR analysis of *NLRP3* and *IL-1β* expression of HLECs following treatment with HG (150 mM) for 4 hours in the absence or presence of NLRP3 inflammasome inhibitor MCC950 (1 µm) pretreated for 1 hour. (**C**, **D**) HLECs were treated as indicated for 24 hours, and cell lysates were subjected to immunoblotting with antibodies against NLRP3, IL-1β, IL-1β p17, and GAPDH. (**E**) Cell viability of indicated HLECs following treatment with HG with or without NLRP3 inhibitor MCC950 for 1 hour. The cell viability was assessed using the CCK8 kit, with results expressed as the percentage of CCK8 reduction. (**G**) Representative immunofluorescence images of indicated HLECs against ASC. The *white arrows* indicate ASC speckles. (**F**, **H**) Bright-field and PI staining images of indicated HLECs treated with HG in the absence or presence of MCC950 for 1 hour. The total percentage of dead cells was determined and quantified by PI staining. Data were collected from three separate experiments. $^{*}P < 0.05$, $^{**}P < 0.01$, $^{***}P < 0.001$; ns, not significant.

(Figs. 5I, 5J). These results suggest that SIRT1 plays an upstream inhibitory role in HG-induced TXNIP/NLRP3 inflammasome activation.

To confirm and extend these results, we tested the effects of SRT1720, a SIRT1 agonist, on NLRP3 inflammasome activation. Culturing in HG (150 mM) medium increased mRNA and protein levels of TXNIP and NLRP3 and protein levels of ASC, IL-1β, and IL-1β p17 secretion ($P \leq 0.013$), and SRT1720 treatment reversed these increases, nearly to their baseline levels (Figs. 6A–E). ROS generation also followed the above changes (Fig. 6H). Cell viability and PI results showed a significant protective effect of SRT1720 on HG-induced cell death ($P = 0.026$) (Figs. 6F–H). Thus, the selective SIRT1 agonist SRT1720 is also a viable option to treat TXNIP/NLRP3 inflammasome-associated inflammation under HG stress.

SIRT1/TXNIP/NLRP3 Pathway Involved in HG-Induced Cataractogenesis in Rat Lenses

The above results indicate that SIRT1 plays an inhibitory role on TXNIP/NLRP3 inflammasome activation, so we conducted lens culture experiments to assess whether rat

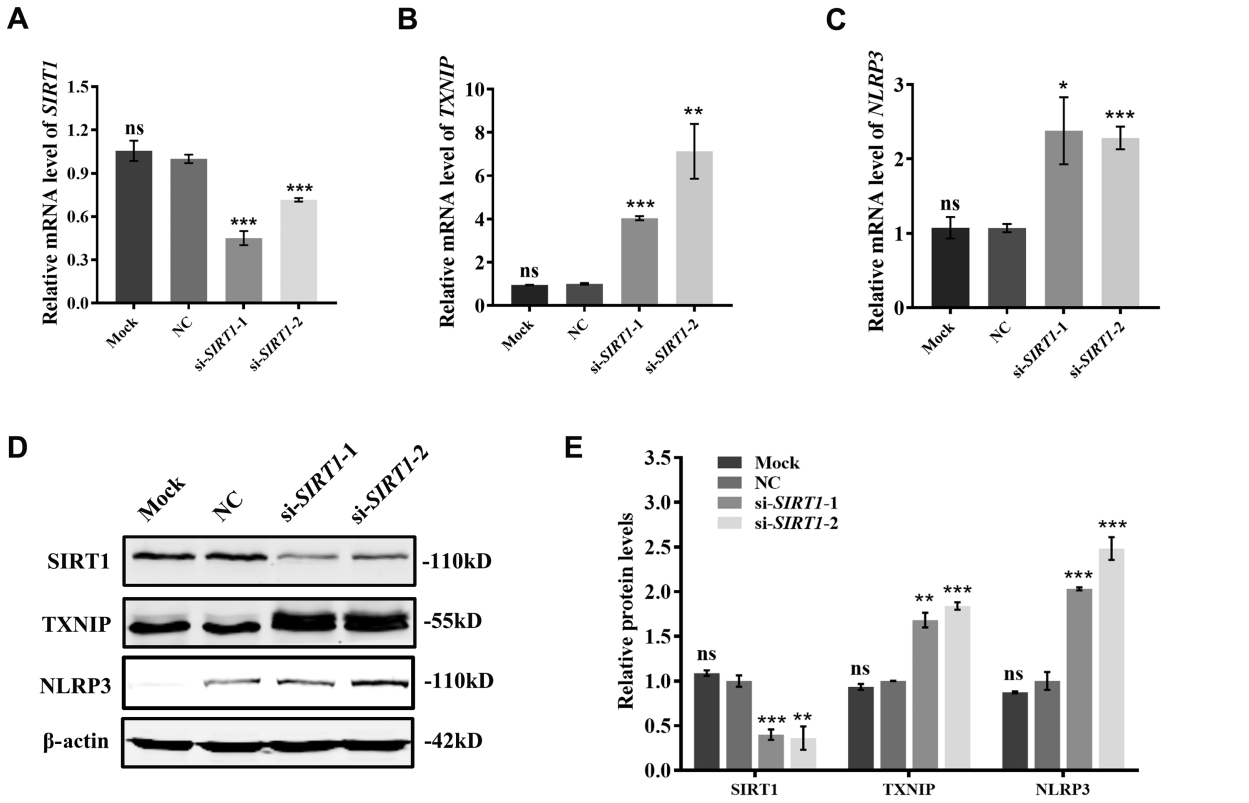

Figure 4. Effect of knockdown of SIRT1 on TXNIP/NLRP3 activity. (**A–C**) qRT-PCR analysis of *SIRT1*, *TXNIP*, and *NLRP3* expression in HLECs transfected with control or *SIRT1* siRNAs for 48 hours. (**D**) HLECs were transfected with control or NLRP3 siRNAs for 72 hours. Cells were lysed and immunoblotted with antibodies against SIRT1, TXNIP, NLRP3, and β-actin. (**E**) Quantification of protein levels based on the indicated Western blot analysis. Data were collected from three separate experiments. $^{*}P < 0.05$, $^{**}P < 0.01$, $^{***}P < 0.001$; ns, not significant, as compared with the 5.5-mM glucose group.

lenses develop cataracts under HG stress and, if so, whether an NLRP3 inhibitor or SIRT1 agonist could suppress the process. Lenses were extracted from 4-week-old rats and cultivated in 150 mM glucose or 150 mM mannitol media for 7 days. Except for an insignificant increase of cortex density on day 7, the high mannitol–treated lenses showed similar clarity as the normal control group in the first 5 days (Figs. 7A, 7B). The lenses in the HG group presented obvious opacities at the peripheral cortex on day 3, which extended to the lens nucleus by day 5, and the lenses turned totally opaque by day 7 (Figs. 7A, 7B). Interestingly, the addition of MCC950 or SRT1720 to the HG-stressed lenses largely reversed cataract formation on day 3. On day 5, the lenses were also nearly transparent ($P \leq 0.002$), and on day 7, only mild opacities were observed in the peripheral cortex (Figs. 7A, 7B). ROS generation was increased in the lens epithelium under HG stress ($P < 0.001$), and both MCC950 and SRT1720 decreased the increase effectively ($P \leq 0.014$) (Figs. 7C, 7E); the TUNEL test also demonstrated that culturing in HG medium resulted in cell apoptosis of the lens epithelial cells, and this was effectively reduced by both MCC950 and SRT1720 treatment ($P \leq 0.001$) (Figs. 7D, 7E).

PCR analysis of the rat lens epithelial cells showed that *SIRT1* mRNA level declined in the HG-stressed lenses ($P < 0.001$), which was reversed by treatment with SRT1720 ($P = 0.003$) (Fig. 8A). In contrast, *TXNIP*, *NLRP3*, and *IL-1β* mRNA levels were significantly elevated by HG stress, and this effect was also significantly reduced by SRT1720 ($P = 0.032$) (Figs. 8B–D). MCC950, an inhibitor of NLRP3, decreased *TXNIP* mRNA levels significantly, but to a lesser extent than SRT1720, and only nominally decreased *IL-1β* mRNA levels (Figs. 8B, 8D). Immunofluorescence analysis of lens sections showed that changes in protein expressions in lens epithelia generally corresponded to their mRNA levels. NLRP3 protein expression increased under HG stress but was reduced to a normal level when treated with MCC950 or SRT1720; SIRT1 protein levels were decreased by HG stress but returned to baseline levels by coculturing with SRT1720 but not MCC950; TXNIP protein levels were increased by culture in HG media but decreased in both MCC950- and SRT1720-treated lens epithelial cells; finally, IL-1β protein expression increased under HG stress, but was also decreased slightly in the lenses treated with MCC950 and more significantly with SRT1720 treatment (Fig. 8E). These results suggest that SIRT1 agonists may have a better effect on inhibiting TXNIP/NLRP3 inflammasome-associated inflammation than the NLRP3 inhibitor, since SIRT1 agonists more significantly suppresses both TXNIP and NLRP3 expressions.

Discussion

Diabetic cataract is a major threat to vision in patients with DM because of its high risk of premature and rapid progression. Surgery currently is the only way to remove cataracts, but patients with DM are more vulnerable to postoperative complications, including endophthalmitis

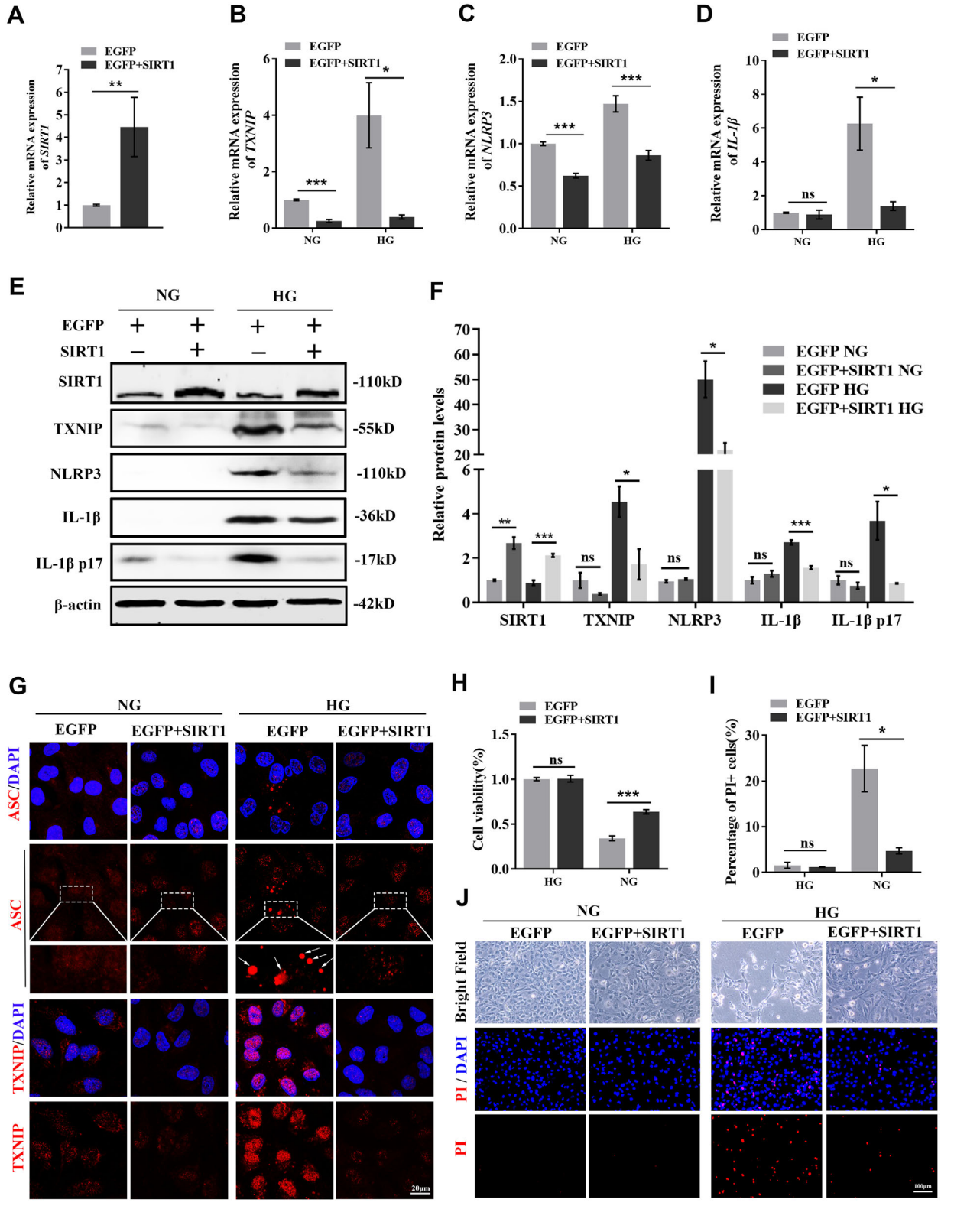

Figure 5. Overexpression of SIRT1 suppresses TXNIP/NLRP3 inflammasome activation. (**A**) HLECs were infected with control and SIRT1 overexpression lentiviruses and then subjected to qRT-PCR analysis of SIRT1. (**B–D**) qRT-PCR was performed to assess mRNA expression of *TXNIP*, *NLRP3*, and *IL-1β* in control and *SIRT1* overexpressing HLECs treated with HG (150 mM) for 4 hours. (**E**, **F**) Expression of SIRT1 and TXNIP/NLRP3 inflammasome-associated proteins was detected in the indicated overexpressing HLECs treated with HG as indicated for 24 hours using WB. (**G**) Representative images of immunostaining of indicated overexpression HLECs treated with HG for 24 hours detected by anti-ASC and anti-TXNIP antibodies. *White arrows* indicate ASC speckles. (**H**) Cell viability of indicated lentivirus-infected HLECs following treatment with HG for 24 hours. (**I**, **J**) Bright-field and PI staining images of indicated lentivirus-infected HLECs treated with HG for 24 hours. The total percentage of dead cells was determined and quantified by PI staining. Data were collected from three separate experiments. $^{*}P < 0.05$, $^{**}P < 0.01$, $^{***}P < 0.001$.

Investigative Ophthalmology & Visual Science

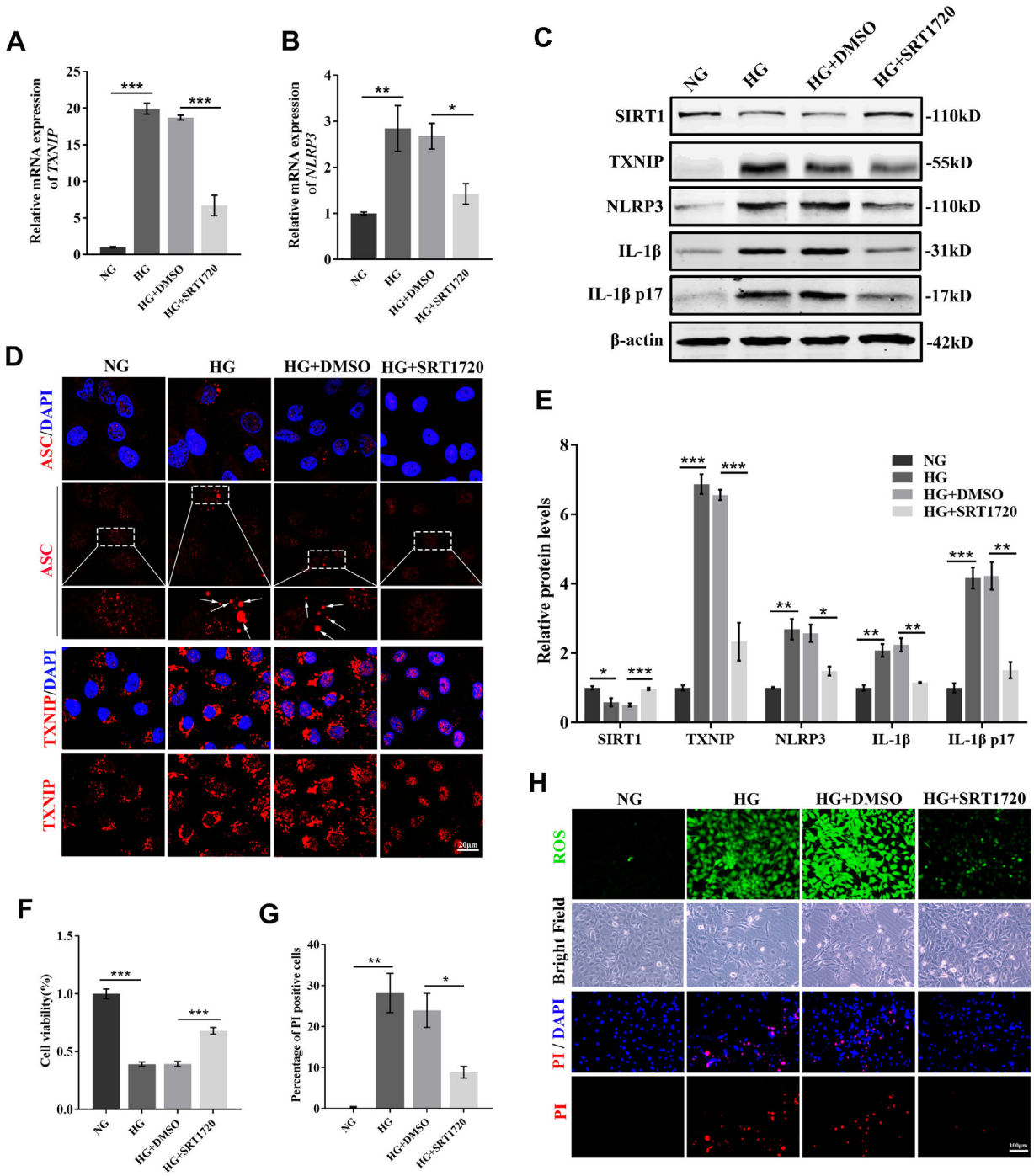

Figure 6. SRT1720 rescues HG-induced HLEC pyroptosis. Schematic representation of SRT1720 treatment experiments. (**A**, **B**) qRT-PCR analysis of *TXNIP* and *NLRP3* expression of HLECs following treatment with HG (150 mM) for 4 hours in the absence or presence of SIRT1 agonist SRT1720 (0.5 μm) pretreated for 1 hour. (**C**, **E**) Quantification of SIRT1, TXNIP, NLRP3, IL-1β, and IL-1β p17 levels from HLECs treated with HG (150 mM) for 24 hours in the absence or presence of SRT1720 pretreated for 1 hour in WB. (**D**) Representative images of immunostaining of indicated HLECs treated with HG and SRT1720 detected by anti-ASC and anti-TXNIP antibodies. *White arrows* indicate ASC speckles. (**F–H**) Cell viability and PI staining images and statistic results of indicated HLECs treated with HG and SRT1720, as well as representative images of ROS generation and bright-field. Data were collected from three separate experiments. $^{*}P < 0.05$, $^{**}P < 0.01$, $^{***}P < 0.001$.

and corneal endothelitis,[19,20] which can lead to blindness and pose a heavy burden on the health care system. There has been no effective medication to prevent or delay DC to date, in part because of the complicated underlying mechanism. Our results illustrate that TXNIP/NLRP3 inflammasome-associated inflammation and pyroptosis contribute to HG-induced injuries in HLECs and rat lens epithelia, and SIRT1 is an upstream negative regulator that inhibits the TXNIP/NLRP3 inflammasome pathway. These findings are of potential clinical significance since they

Investigative Ophthalmology & Visual Science

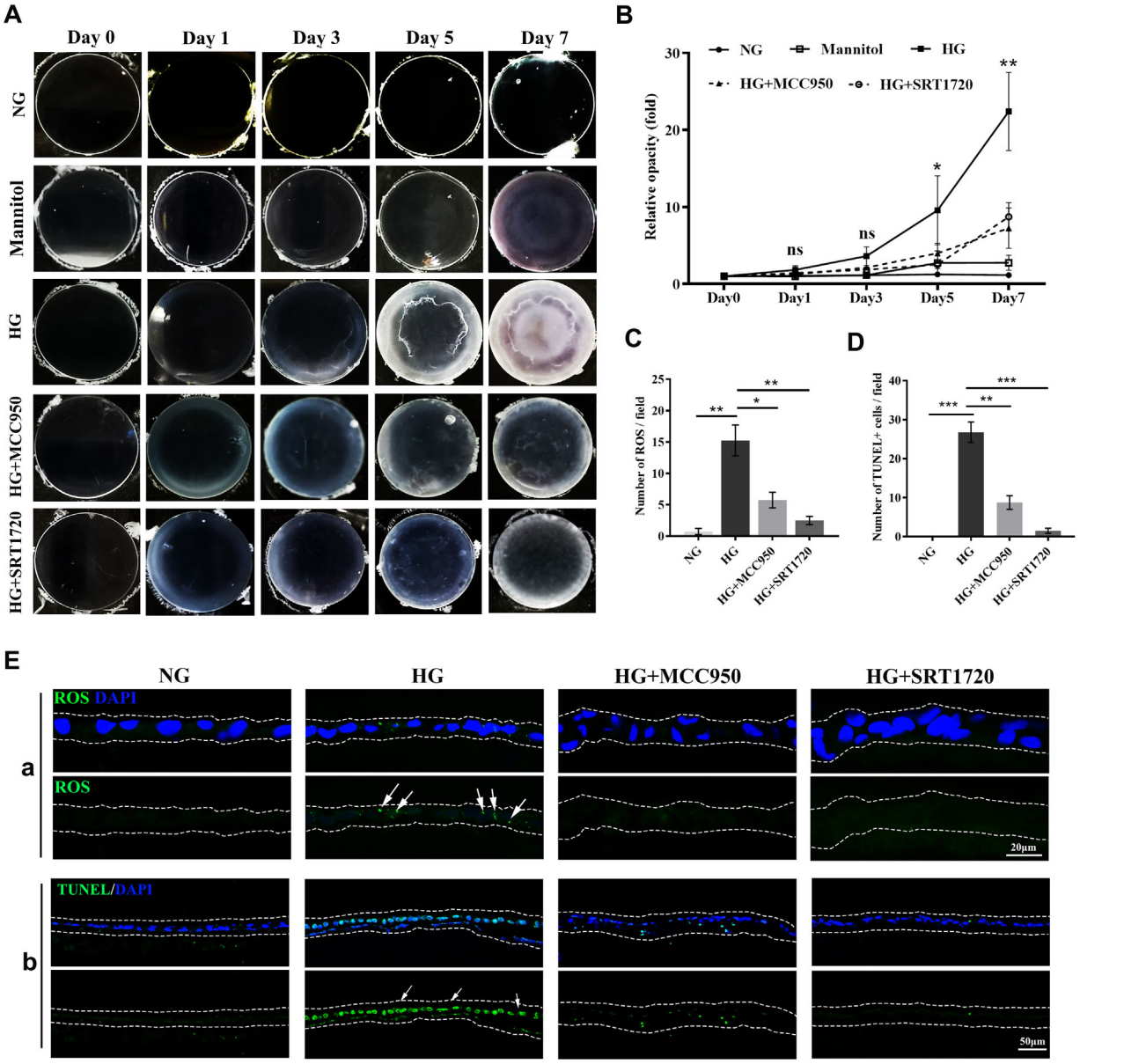

Figure 7. Effect of MCC950 and SRT1720 on HG-induced cataractogenesis in rat lens. (**A**, **B**) Rat lenses ($n = 4$/group) were extracted and cultivated in 150 mM glucose or 150 mM mannitol media for 7 days. High mannitol treatment did not cause significant lens opacity except for an insignificant increase of cortex density on day 7, while the lenses in the HG group started to become opaque at the peripheral cortex on day 3 and showed a total cataract by day 7. The addition of MCC950 or SRT1720 to the HG-stressed lenses prevented the formation of cataracts. (**C–E**) ROS generation and cell apoptosis increased significantly in the lens epithelium under HG stress, and MCC950 or SRT1720 rescued them effectively. Data were collected from four separate experiments. *$P < 0.05$, **$P < 0.01$, ***$P < 0.001$.

suggest potential mechanism-based drug therapies for DC treatment.

The NLRP3 inflammasome plays a significant role in regulating immune inflammatory responses in DM and diabetic complications.[21–23] NLRP3-associated genes and stress markers are upregulated in clinical vitreous and retina samples from patients with diabetic retinopathy,[24] and drugs that decrease NLRP3 inflammasome activation are able to suppress hyperglycemia-induced retinal inflammation in diabetic animal models.[25] The mechanisms controlling the undesired inflammasome activation are of great interest, for they hold the potential to prevent or terminate inflammasome overactivation and maintain homeostasis. However, the candidates for DC treatment are currently very limited. The current study shows that SIRT1 is a powerful negative regulator of TXNIP/NLRP3 inflammasome activation, which is a novel finding for understanding the molecular mechanisms controlling NLRP3 inflammasome activation in DC. SIRT1 agonists provide a stronger and more general inhibitory effect than the NLRP3 inhibitor on NLRP3 inflammasome-induced inflammation and cataract development, for they suppress expressions of both TXNIP and NLRP3.

TXNIP, an ROS sensor and an endogenous inhibitor of the antioxidant thioredoxin, acts as a binding partner of NLRP3.[26] In the presence of ROS, TXNIP releases

Investigative Ophthalmology & Visual Science

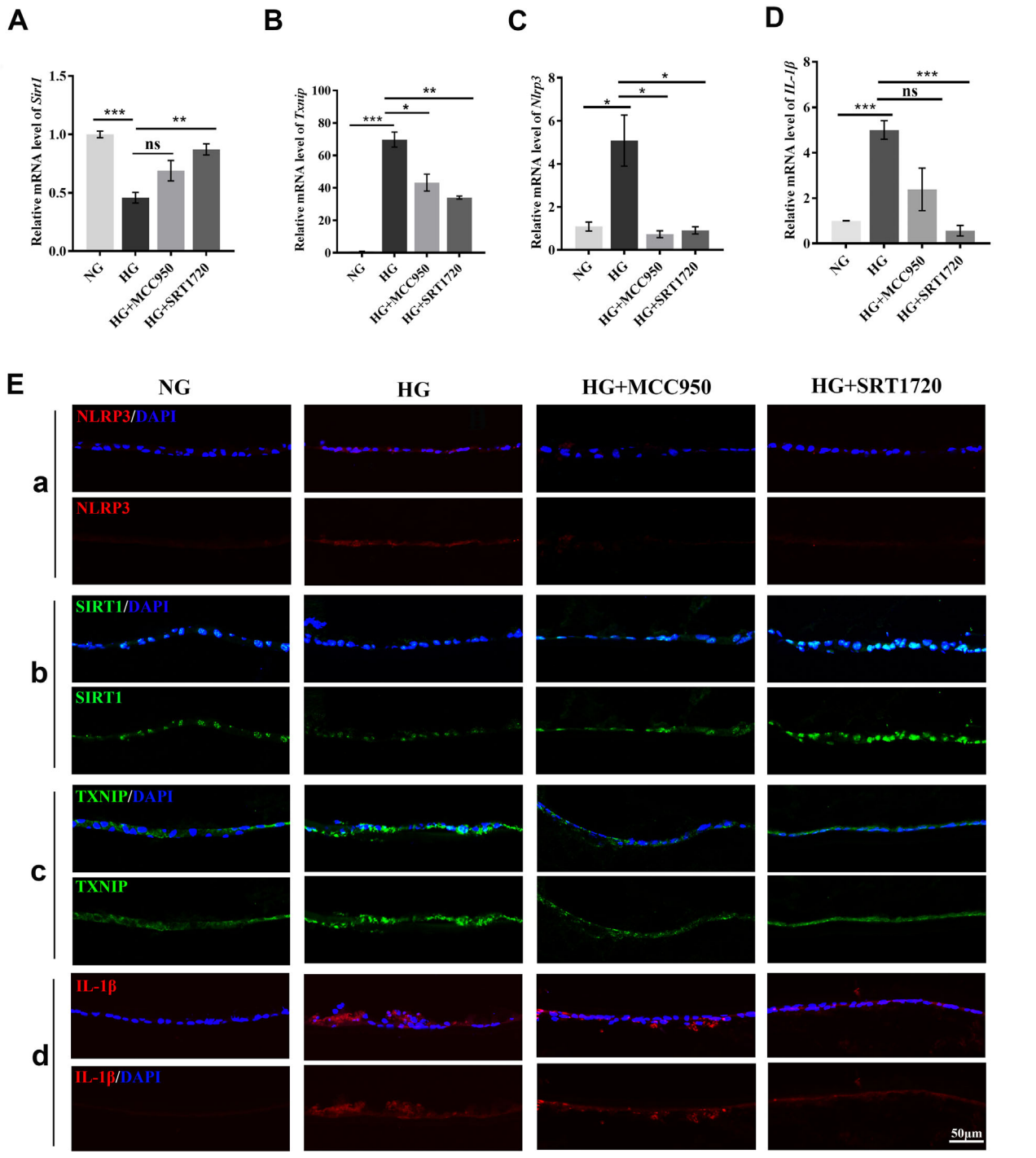

Figure 8. Effects of MCC950 and SRT1720 on SIRT1/TXNIP/NLRP3 pathway in HG-stressed rat lenses. (**A–D**) mRNA levels of *SIRT1* declined in the HG-stressed lens capsules, which was prevented by treatment with SRT1720 but not MCC950. The increases in *TXNIP*, *NLRP3*, and *IL-1β* mRNA levels were significantly reduced by SRT1720 treatment, and MCC950 showed less effect. (**E**) Immunofluorescence results show that their protein expressions in the lens capsule/epithelia correspond to their transcriptional levels. Data were collected from four separate experiments. $^{*}P < 0.05$, $^{**}P < 0.01$, $^{***}P < 0.001$.

from thioredoxin, which can fulfill its redox signaling functions such as reduction of oxidized cysteine residues and the cleavage of disulfide bonds, and itself participates in NLRP3 inflammasome activation, which involves two steps: priming and inflammasome assembly.[27] Before assembly, interaction of TXNIP and NLRP3 is essential for subsequent recruitment of ASC and inflammasome activation.[16] The combination of the TXNIP/NLRP3 inflammasome is widely observed in diabetic complications,[28] such as diabetic retinopathy and diabetic nephropathy.[29,30] It was reported that TXNIP mediates hyperglycemia/ROS-induced NLRP3 inflammasome activation and pyroptosis,[17] while knockdown of TXNIP suppressed its binding to NLRP3 and the subsequent inflammasome assembly and IL-1β secretion.[26] Although TXNIP was suggested as a promising therapeutic target, there is currently a lack

Investigative Ophthalmology & Visual Science

of known specific pharmacologic inhibitors. Our results provided support for SIRT1 as a candidate for the inhibition of both TXNIP and NLRP3, which could be more effective than a single inhibitor acting on either one individually.

SIRT1 plays important roles in the regulation of cell survival, apoptosis, and inflammation,[9] as well as in insulin signaling pathways, acting as a sensor and protector of the redox environment.[31] It is an NAD-dependent deacetylase and regulates protein function through deacetylation of lysine residues. It has been reported that SIRT1 protects mesenchymal stem cells from radiation damage by inhibiting NLRP3 inflammasome-induced IL-1β release.[32] It is also possible that SIRT1 mediates inhibition of NLRP3 inflammasome activation via deacetylating NF-$\kappa\beta$, which targets TXNIP and NLRP3.[33] Our current results show that in HG-stressed HLECs, SIRT1 plays a negative regulatory role on TXNIP/NLRP3 inflammasome-associated inflammation and cell pyroptosis, which correlates with its effects in preventing cataract formation in rat lenses cultured in HG medium. Finally, as a versatile deacetylase, SIRT1 affects a variety of substrates, including p53, another transcription factor that targets ASC, which is required for NLRP3 inflammasome assembly.[34] Consistent with this, our results also show that ASC expression increases under HG stress, which can be reversed by MCC950, SRT1720 treatment, or LV-SIRT1 transfection. However, it is also quite possible that SIRT1 was not the only upstream regulator of HG-induced TXNIP/NLRP3 inflammasome activation, since our results demonstrated that SIRT1 overexpression could significantly decrease but not totally prevent the inflammasome activation and the subsequent IL-1β p17 secretion. Transient receptor potential melastatin 2 was previously found as another contributor regulating HG-induced ROS generation and TXNIP/NLRP3 inflammasome activation via p47 phox activation in human monocytes.[35] Thus, the real signal pathways involved in the inflammasome regulation were probably a complicated network rather than a simple linear domination.

Admittedly, our results would be more strengthened if data from DC animal models was available. DM is a systematic autoimmune disease, which means that it is not comprehensive to understand the pathologic mechanism of diabetic complications such as DC if we overlooked the surrounding tissues of the lens, such as zonulas, ciliary body, aqueous humor, and vitreous. It was reported that a variety of immune cells might travel from the ciliary body to the lens via the zonulas to cause cataractogenesis, in response to oxidative stress or other injuries.[36,37] Thus, the SIRT1/TXNIP/NLRP3 inflammasome pathway in the surrounding tissues in a DC animal model needs to be explored in our further studies. Besides, the comparisons between SIRT1 agonists and the known cataract drugs, such as resveratrol, which delays the progression of DC partially through suppressing oxidative damage,[38] could be carried out both in vitro and in vivo to provide stronger evidence for their potential clinical application.

Taken together, our results show that the TXNIP/NLRP3 inflammasome pathway leads to HG-induced inflammation and pyroptosis in HLECs and cultured rat lenses. SIRT1 is a powerful negative regulator of this inflammasome activation, which will help to identify new inhibitors to suppress the inflammasome-associated inflammation and provide possible strategies to treat DC.

Acknowledgments

Supported by research grants from the Natural Science Foundation of Zhejiang Province (LY20H120006 to YR) and the National Natural Science Foundation of China (82070932 to QZ; 82171065 to XM).

Disclosure: **L. Lian**, None; **Z. Le**, None; **Z. Wang**, None; **Y. Chen**, None; **X. Jiao**, None; **H. Qi**, None; **J.F. Hejtmancik**, None; **X. Ma**, None; **Q. Zheng**, None; **Y. Ren**, None

References

1. Saxena S, Mitchell P, Rochtchina E. Five-year incidence of cataract in older persons with diabetes and pre-diabetes. *Ophthalmic Epidemiol*. 2004;11(4):271–277.
2. Chan G, Tang SC. Current practices in the management of diabetic nephropathy. *J R Coll Physicians Edinb*. 2013;43(4):330–332; quiz 333.
3. Ott C, Jacobs K, Haucke E, Navarrete Santos A, Grune T, Simm A. Role of advanced glycation end products in cellular signaling. *Redox Biol*. 2014;2:411–429.
4. Lima J, Moreira NCS, Sakamoto-Hojo ET. Mechanisms underlying the pathophysiology of type 2 diabetes: From risk factors to oxidative stress, metabolic dysfunction, and hyperglycemia. *Mutat Res Genet Toxicol Environ Mutagen*. 2022;874–875:503437.
5. Obrosova IG, Chung SS, Kador PF. Diabetic cataracts: Mechanisms and management. *Diabetes Metab Res Rev*. 2010;26(3):172–180.
6. Lledó VE, Alkozi HA, Sánchez-Naves J, Fernandez-Torres MA, Guzman-Aranguez A. Melatonin counteracts oxidative damage in lens by regulation of Nrf2 and NLRP3 inflammasome activity. *Exp Eye Res*. 2022;215:108912.
7. Marneros AG. Increased VEGF-A promotes multiple distinct aging diseases of the eye through shared pathomechanisms. *EMBO Mol Med*. 2016;8(3):208–231.
8. Yang T, Fu M, Pestell R, Sauve AA. SIRT1 and endocrine signaling. *Trends Endocrinol Metab*. 2006;17(5):186–191.
9. Singh V, Ubaid S. Role of silent information regulator 1 (SIRT1) in regulating oxidative stress and inflammation. *Inflammation*. 2020;43(5):1589–1598.
10. Rodgers JT, Lerin C, Haas W, Gygi SP, Spiegelman BM, Puigserver P. Nutrient control of glucose homeostasis through a complex of PGC-1alpha and SIRT1. *Nature*. 2005;434(7029):113–118.
11. Zeng K, Feng QG, Lin BT, Ma DH, Liu CM. Effects of microRNA-211 on proliferation and apoptosis of lens epithelial cells by targeting SIRT1 gene in diabetic cataract mice. *Biosci Rep*. 2017;37(4):BSR20170695.
12. Bai R, Lang Y, Shao J, Deng Y, Refuhati R, Cui L. The role of NLRP3 inflammasome in cerebrovascular diseases pathology and possible therapeutic targets. *ASN Neuro*. 2021;13:17590914211018100.
13. Jiang T, Jiang D, Zhang L, Ding M, Zhou H. Anagliptin ameliorates high glucose–induced endothelial dysfunction via suppression of NLRP3 inflammasome activation mediated by SIRT1. *Mol Immunol*. 2019;107:54–60.
14. Li H, Li R, Wang L, Liao D, Zhang W, Wang J. Proanthocyanidins attenuate the high glucose-induced damage of retinal pigment epithelial cells by attenuating oxidative stress and inhibiting activation of the NLRP3 inflammasome. *J Biochem Mol Toxicol*. 2021;35(9):e22845.
15. Jiang T, Gu J, Chen W, Chang Q. Resveratrol inhibits high-glucose-induced inflammatory "metabolic memory" in human retinal vascular endothelial cells through SIRT1-dependent signaling. *Can J Physiol Pharmacol*. 2019;97(12):1141–1151.

16. Zhou R, Tardivel A, Thorens B, Choi I, Tschopp J. Thioredoxin-interacting protein links oxidative stress to inflammasome activation. *Nat Immunol*. 2010;11(2):136–140.
17. Schroder K, Zhou R, Tschopp J. The NLRP3 inflammasome: A sensor for metabolic danger? *Science*. 2010;327(5963):296–300.
18. Dai X, Liao R, Liu C, et al. Epigenetic regulation of TXNIP-mediated oxidative stress and NLRP3 inflammasome activation contributes to SAHH inhibition-aggravated diabetic nephropathy. *Redox Biol*. 2021;45:102033.
19. Park J, Popovic MM, Balas M, El-Defrawy SR, Alaei R, Kertes PJ. Clinical features of endophthalmitis clusters after cataract surgery and practical recommendations to mitigate risk: Systematic review. *J Cataract Refract Surg*. 2022;48(1):100–112.
20. Wang H, Zheng J, Zheng Q, et al. Incidence and risk factors of new onset endotheliitis after cataract surgery. *Invest Ophthalmol Vis Sci*. 2018;59(12):5210–5216.
21. Charlton A, Garzarella J, Jandeleit-Dahm KAM, Jha JC. Oxidative stress and inflammation in renal and cardiovascular complications of diabetes. *Biology (Basel)*. 2020;10(1):18.
22. Yu ZW, Zhang J, Li X, Wang Y, Fu YH, Gao XY. A new research hot spot: The role of NLRP3 inflammasome activation, a key step in pyroptosis, in diabetes and diabetic complications. *Life Sci*. 2020;240:117138.
23. Chen H, Zhang X, Liao N, et al. Enhanced expression of NLRP3 inflammasome-related inflammation in diabetic retinopathy. *Invest Ophthalmol Vis Sci*. 2018;59(2):978–985.
24. Chen H, Zhang X, Liao N, et al. Identification of NLRP3 inflammation-related gene promoter hypomethylation in diabetic retinopathy. *Invest Ophthalmol Vis Sci*. 2020;61(13):12.
25. Thounaojam MC, Montemari A, Powell FL, et al. Monosodium urate contributes to retinal inflammation and progression of diabetic retinopathy. *Diabetes*. 2019;68(5):1014–1025.
26. Abais JM, Xia M, Li G, et al. Nod-like receptor protein 3 (NLRP3) inflammasome activation and podocyte injury via thioredoxin-interacting protein (TXNIP) during hyperhomocysteinemia. *J Biol Chem*. 2014;289(39):27159–27168.
27. Nakajo T, Katayoshi T, Kitajima N, Tsuji-Naito K. 1,25-Dihydroxyvitamin D(3) attenuates IL-1β secretion by suppressing NLRP1 inflammasome activation by upregulating the NRF2-HO-1 pathway in epidermal keratinocytes. *Redox Biol*. 2021;48:102203.
28. Amin FM, Abdelaziz RR, Hamed MF, Nader MA, Shehatou GSG. Dimethyl fumarate ameliorates diabetes-associated vascular complications through ROS-TXNIP-NLRP3 inflammasome pathway. *Life Sci*. 2020;256:117887.
29. Du J, Wang Y, Tu Y, et al. A prodrug of epigallocatechin-3-gallate alleviates high glucose-induced pro-angiogenic factor production by inhibiting the ROS/TXNIP/NLRP3 inflammasome axis in retinal Müller cells. *Exp Eye Res*. 2020;196:108065.
30. Han Y, Xu X, Tang C, et al. Reactive oxygen species promote tubular injury in diabetic nephropathy: The role of the mitochondrial ros-txnip-nlrp3 biological axis. *Redox Biol*. 2018;16:32–46.
31. Haigis MC, Sinclair DA. Mammalian sirtuins: Biological insights and disease relevance. *Annu Rev Pathol*. 2010;5:253–295.
32. Fu Y, Wang Y, Du L, et al. Resveratrol inhibits ionising irradiation-induced inflammation in MSCs by activating SIRT1 and limiting NLRP-3 inflammasome activation. *Int J Mol Sci*. 2013;14(7):14105–14118.
33. Zhou Y, Wang S, Wan T, et al. Cyanidin-3-O-β-glucoside inactivates NLRP3 inflammasome and alleviates alcoholic steatohepatitis via SirT1/NF-κB signaling pathway. *Free Radic Biol Med*. 2020;160:334–341.
34. Huang Y, Yong P, Dickey D, Vora SM, Wu H, Bernlohr DA. Inflammasome activation and pyroptosis via a lipid-regulated SIRT1-p53-ASC axis in macrophages from male mice and humans. *Endocrinology*. 2022;163(4):bqac014.
35. Tseng HH, Vong CT, Kwan YW, Lee SM, Hoi MP. TRPM2 regulates TXNIP-mediated NLRP3 inflammasome activation via interaction with p47 phox under high glucose in human monocytic cells. *Sci Rep*. 2016;6:35016.
36. Menko AS, Walker JL, Stepp MA. Fibrosis: Shared lessons from the lens and cornea. *Anat Rec (Hoboken)*. 2020;303(6):1689–1702.
37. Logan CM, Bowen CJ, Menko AS. Induction of immune surveillance of the dysmorphogenic lens. *Sci Rep*. 2017;7(1):16235.
38. Higashi Y, Higashi K, Mori A, Sakamoto K, Ishii K, Nakahara T. Anti-cataract effect of resveratrol in high-glucose-treated streptozotocin-induced diabetic rats. *Biol Pharm Bull*. 2018;41(10):1586–1592.

Investigative Ophthalmology & Visual Science